METAL–OLEFIN BONDING. X-RAY STRUCTURES OF TRICHLORO-1,6-BIS(DIPHENYLPHOSPHINO)-*trans*-HEX-3-ENERHODIUM(III) AND DICHLOROCARBONYL-1,6-BIS(DIPHENYLPHOSPHINO)-*trans*-HEX-3-ENERUTHENIUM(II)

GEORGE R. CLARK* and KAREN MARSDEN

Department of Chemistry, University of Auckland, Auckland (New Zealand)

(Received November 15th, 1983)

Summary

X-ray structures have been determined for the olefin-containing complexes $RuCl_3(BDPH)$ and $RuCl_2(CO)(BDPH)$; BDPH = 1,6-bis(diphenylphosphino)-*trans*-hex-3-ene. Both compounds crystallise in space group *Pbca* with eight molecules in unit cells of dimensions $RhCl_3(BDPH)$ *a* 16.109(8), *b* 20.359(12), *c* 17.194(4) Å; $RuCl_2(CO)(BDPH)$ *a* 16.279(1), *b* 20.160(1), *c* 17.334(1) Å. Least-squares refinement returned residuals, *R*, of 0.030 and 0.067 respectively. In the ruthenium complex the CO and one Cl ligand are statistically interchanged. Both complexes are characterised by weak metal–olefin bonding and a twisted olefin orientation. The geometries are compared with those in other Ir^I and Ir^{III} complexes containing the BDPH ligand.

Introduction

Metal complexes containing tertiary unsaturated phosphines are of interest because of their close relationship to catalysts employed in homogeneous hydrogenation, isomerization, and hydroformylation reactions of olefins. The ligand 1,6-bis(diphenylphosphino)-*trans*-hex-3-ene (BDPH) undergoes normal substitution reactions with iridium(I) and rhodium(I) compounds to form square-planar complexes of general formula MX(BDPH), M = Ir or Rh, X = halide [1]. A crystal structure determination of IrCl(BDPH) confirmed the tridentate nature of the olefin, and showed that the ligand as a whole was sufficiently flexible to allow the olefin to adopt an orientation approximately perpendicular to the square coordination plane [2].

Oxidative addition of H_2, Cl_2, HCl to the above complexes forms octahedral M^{III} species, with nuclear magnetic resonance data indicating considerable weakening of the metal–olefin bonding [2,3]. In the crystal structure of $IrH_2Cl(BDPH)$, the olefin

was found to be extremely weakly bound to Ir, and it adopted an orientation approximately midway between the two expected geometries. These effects were attributed to either reduced metal–olefin $\pi^\star$ backbonding appropriate to the higher oxidation state of the metal (i.e. Ir[III] as opposed to Ir[I]), or to the strong *trans* influence of the hydride ligand, or to both. Subsequent analyses of $IrCl_3(BDPH)$ [3] and $Mo(CO)_3(BDPH)$ [4] showed that their olefins were also twisted, although not by as much as in $IrH_2Cl(BDPH)$.

In order to further investigate the nature of the metal–olefin bonding in these and related complexes we have determined the crystal structures of $RhCl_3(BDPH)$ and $RuCl_2(CO)(BDPH)$. The crystals in fact are nearly isostructural, but as the primary purpose was to detect small differences in geometry within the coordination spheres, both structures have been solved and refined independently.

Experimental

Preliminary X-ray photography showed that the crystals of both compounds belonged to the orthorhombic system with systematic absences ($0\ k\ l$, $k = 2n + 1$; $h\ 0\ l$, $l = 2n + 1$; $h\ k\ 0$, $h = 2n + 1$) characteristic of space group *Pbca*. Suitable crystals were mounted on fine glass fibres and positioned on a Nonius CAD-4 diffractometer. Unit cell dimensions were derived from least-squares fits to the setting angles of twenty-five reflections, using Ni-filtered copper K_α radiation.

Intensity data collections employed the $2\theta/\omega$ scan technique with a total background/peak count time ratio of $1/2$. The omega scan angle was $0.70 + 0.35 \tan \theta$. Reflections were counted for either 80 s or else until $\sigma(I)/I$ was 0.022 [5]. Crystal alignment and decomposition were monitored throughout the data collections by remeasuring three selected standard reflections after every 100 measurements, however no non-statistical variations were recorded. Attenuators were not required. The data were corrected for Lorentz, polarization and absorption effects, and equivalent reflections were averaged [6]. Details of crystal data and intensity data collection procedures are summarised in Table 1.

Structure determinations and refinements

Both structures were solved independently using conventional heavy-atom Patterson and electron density maps, and refined by full-matrix least-squares procedures. Atomic scattering factors and dispersion corrections were from standard listings [7]. The function minimised was $\Sigma w(|F_o| - |F_c|)^2$, with weights w being $4F_o^2/\sigma^2(F_o^2)$ [8]. Residuals quoted are $R = \Sigma(|F_o| - |F_c|)/\Sigma|F_o|$ and $R_w = \{\Sigma_w(|F_o| - |F_c|)^2/\Sigma|F_o|^2\}^{1/2}$.

(a) RhCl_3(BDPH)

All non-hydrogen atoms were located from initial Patterson and electron density maps. Two full-matrix least-squares cycles were computed using isotropic temperature factors for all atoms, followed by two cycles in which the Rh, P and Cl atoms were assigned anisotropic thermal parameters. The R factor was then 0.049.

An analysis of the weighting scheme at this stage showed that the more intense reflections were being heavily weighted compared with those of lower intensity, suggesting that the p factor should be increased. Furthermore, F_c appeared to be systematically larger than F_o for the strong reflections, indicating the need to correct for the effects of secondary extinction. Accordingly, the p factor was changed from

TABLE 1

SUMMARY OF CRYSTAL DATA AND INTENSITY DATA COLLECTIONS FOR $RhCl_3(BDPH)$ AND $RuCl_2(CO)(BDPH)$

	$RhCl_3(BDPH)$	$RuCl_2(CO)(BDPH)$
Formula	$C_{30}H_{30}Cl_3P_2Rh$	$C_{31}H_{30}Cl_2OP_2Ru$
Molecular weight	661.74	652.50
Crystal habit and colour	Orange columns	Pale yellow needles
a (Å)	16.109(8)	16.279(1)
b (Å)	20.359(12)	20.160(1)
c (Å)	17.194(4)	17.334(1)
V (Å^3)	5639.0	5688.9
Temperature (K)	293(1)	293(1)
Z	8	8
Space group	$Pbca$ (No. 61)	$Pbca$
ρ_c (g cm^{-3})	1.56	1.52
ρ_o	1.55(2) (KBr)	1.52(2) ($ZnBr_2$)
$F(0\,0\,0)$	2688	2656
Crystal size (mm)	$0.08 \times 0.14 \times 0.20$	$0.08 \times 0.12 \times 0.22$
Boundary faces	$\{0\,1\,0\}$, $\{0\,0\,1\}$,	$\{0\,1\,0\}$, $\{0\,0\,1\}$,
	$(1\,0\,0)$, $(\bar{1}\,1\,1)$	$(2\,0\,1)$, $(\bar{2}\,\bar{1}\,\bar{1})$,
		$(\bar{2}\,1\,\bar{1})$
μ(Cu-K_α) (cm^{-1})	88.50	75.78
Transmission coefficients	0.341–0.716	0.256–0.580
Mosaic spread (°)	0.12	0.17
θ (maximum) (°)	57	60
p factor	0.04 initially, but 0.06 for final refinement cycles	0.06
Total reflections	4244	4212
Observed data	$1644(I > 3\sigma(I))$	2089

0.04 to 0.06, and an extinction coefficient was refined [9]. Two cycles were computed and the weighting checked again. The function $\langle w(|F_o| - |F_c|)^2 \rangle$ was now satisfactorily constant, and remained so throughout subsequent refinement cycles.

Hydrogen atoms of the phenyl rings were included in positions calculated assuming C–H 0.95 Å. The sites of the remaining ten hydrogen atoms were found from a difference electron density map and optimised using the peak interpolation procedure of Booth [10]. Although included in the structure factor calculations, no attempt was made to refine any of the hydrogen atoms. After two final cycles the residuals were $R = 0.030$ and $R_w = 0.038$. The largest parameter shift/error was 0.01, and a final difference map was featureless (the most prominent peak was of height 0.17 e Å^{-3} and was adjacent to a phosphorus atom).

Final atomic positions for $RhCl_3(BDPH)$ are listed in Table 2. Hydrogen atom positions, thermal parameters, and tables of observed and calculated structure factors are available on request from the authors (G.R.C.).

(b) $RuCl_2(CO)(BDPH)$

Atomic positions could be unambiguously assigned for most of the non-hydrogen atoms from Patterson and electron density maps. However, the carbonyl group and one of the chloride ligands were not separately resolved, but appeared as equally-

TABLE 2

ATOMIC POSITIONS FOR RhCl$_3$(BDPH)

Atom	x/a	y/b	z/c
Rh	0.06184(3)	0.01685(3)	0.19126(3)
Cl(1)	0.0127(1)	−0.01326(9)	0.3147(1)
Cl(2)	0.1743(1)	0.07236(9)	0.2507(1)
Cl(3)	0.1081(1)	0.04861(9)	0.0666(1)
P(1)	−0.0124(1)	0.11733(9)	0.2045(1)
P(2)	0.1479(1)	−0.07933(9)	0.1815(1)
C(1)	−0.1101(5)	0.1062(4)	0.1514(5)
C(2)	−0.1308(5)	0.0329(3)	0.1572(5)
C(3)	−0.0595(5)	−0.0041(3)	0.1236(4)
C(4)	−0.0315(4)	−0.0637(4)	0 1511(5)
C(5)	0.0112(5)	−0.1149(4)	0.1039(5)
C(6)	0.0792(5)	−0.1461(4)	0.1510(5)
C(11)	0.0283(5)	0.1947(4)	0.1672(4)
C(12)	−0.0237(5)	0.2489(4)	0.1711(4)
C(13)	0.0034(5)	0.3098(4)	0.1438(5)
C(14)	0.0809(5)	0.3163(4)	0.1165(5)
C(15)	0.1328(5)	0.2629(4)	0.1099(5)
C(16)	0.1078(5)	0.2011(4)	0.1371(5)
C(21)	−0.0429(4)	0.1409(3)	0.3022(4)
C(22)	0.0162(5)	0.1672(4)	0.3514(5)
C(23)	−0.0052(6)	0.1888(4)	0.4255(5)
C(24)	−0.0860(5)	0.1836(4)	0.4499(5)
C(25)	−0.1450(6)	0.1573(4)	0.4029(5)
C(26)	−0.1235(5)	0.1364(4)	0.3283(5)
C(31)	0.2031(5)	−0.1123(4)	0.2657(4)
C(32)	0.2388(6)	−0.1744(4)	0.2568(5)
C(33)	0.2794(6)	−0.2024(5)	0.3202(6)
C(34)	0.2831(6)	−0.1710(4)	0.3900(5)
C(35)	0.2481(6)	−0.1107(4)	0.3989(5)
C(36)	0.2068(5)	−0.0815(4)	0.3363(4)
C(41)	0.2262(4)	−0.0733(3)	0.1046(4)
C(42)	0.2223(5)	−0.1110(4)	0.0361(5)
C(43)	0.2815(5)	−0.1003(4)	−0.0218(5)
C(44)	0.3414(5)	−0.0546(4)	−0.0145(5)
C(45)	0.3465(5)	−0.0174(4)	0.0529(5)
C(46)	0.2887(5)	−0.0268(4)	0.1123(4)

weighted overlapping peaks. The Ru–Cl and Ru–C–O bond lengths are such that when the two are overlapped the chlorine atom falls approximately into the centre of the short C–O bond, and the peaks in the electron density map merge into a single peak. As there was no possibility from the X-ray data of satisfactorily resolving the overlapping peaks into individual atoms, they were placed in positions which afforded the best compromise between typical Ru–Cl and Ru–C–O bond lengths and the observed peak positions. They were assigned individual occupancies of 0.5, and arbitrary isotropic temperature factors of 3.0 or chlorine and 5.0 for carbon and oxygen, and all parameters were fixed throughout the following least-squares refinement cycles.

Other aspects of the refinement were as described for RhCl$_3$(BDPH). In successive stages, the heavier atoms then the carbon atoms of the olefin chain were assigned anisotropic thermal parameters. The twenty hydrogen atoms of the phenyl

rings were included in calculated positions, whereas the hydrogen atoms of the olefin chain were obtained from a difference map. Refinement was terminated when the largest parameter shift per standard deviation was 0.10 and R and R_w were 0.067 and 0.086 respectively. There was no sign of any solvent molecules in any of the difference maps calculated at various stages during the refinement. A weighting scheme analysis confirmed as satisfactory the choice of 0.06 for the p factor.

Final atomic positions for $RuCl_2(CO)(BDPH)$ are listed in Table 3. Hydrogen atom positions, thermal parameters, and tables of observed and calculated structure factors are available on request from the authors (G.R.C.).

TABLE 3

ATOMIC POSITIONS FOR $RuCl_2(CO)(BDPH)$

| Atom	x/a	y/b	z/c
Ru	0.06054(6)	0.01653(5)	0.19291(6)
Cl(1)	0.1752(2)	0.0744(2)	0.2531(2)
P(1)	−0.0148(2)	0.1176(2)	0.2056(2)
P(2)	0.1460(2)	−0.0809(2)	0.1808(2)
C(1)	−0.1103(9)	0.1077(7)	0.1500(9)
C(2)	−0.1300(8)	0.0326(7)	0.1556(9)
C(3)	−0.0591(8)	−0.0042(7)	0.1264(9)
C(4)	−0.0314(8)	−0.0645(7)	0.1527(9)
C(5)	0.0074(10)	−0.1171(8)	0.1059(11)
C(6)	0.0784(10)	−0.1489(8)	0.1517(9)
Cl(2A)	0.0137	−0.0137	0.3203
Cl(2B)	0.1094	0.0469	0.0547
C(7A)	0.0980	0.0490	0.0900
C(7B)	0.0210	−0.0080	0.2900
O(A)	0.1215	0.0800	0.0240
O(B)	0.0000	−0.0270	0.3540
C(11)	0.0251(9)	0.1969(7)	0.1691(8)
C(12)	−0.0261(9)	0.2507(8)	0.1693(10)
C(13)	−0.0014(10)	0.3103(8)	0.1420(11)
C(14)	0.0802(10)	0.3172(8)	0.1149(10)
C(15)	0.1292(10)	0.2624(8)	0.1103(10)
C(16)	0.1042(9)	0.2031(7)	0.1368(9)
C(21)	−0.0466(8)	0.1421(7)	0.3028(9)
C(22)	0.0144(9)	0.1664(8)	0.3517(10)
C(23)	−0.0075(11)	0.1864(8)	0.4275(11)
C(24)	−0.0867(11)	0.1832(8)	0.4484(10)
C(25)	−0.1467(11)	0.1587(8)	0.4035(11)
C(26)	−0.1275(10)	0.1373(8)	0.3267(9)
C(31)	0.2020(9)	−0.1161(7)	0.2641(9)
C(32)	0.2361(11)	−0.1784(8)	0.2564(11)
C(33)	0.2733(12)	−0.2096(10)	0.3189(12)
C(34)	0.2826(10)	−0.1721(8)	0.3865(10)
C(35)	0.2481(11)	−0.1134(9)	0.3955(11)
C(36)	0.2076(9)	−0.0839(7)	0.3342(9)
C(41)	0.2221(8)	−0.0746(7)	0.1036(9)
C(42)	0.2206(10)	−0.1145(8)	0.0376(10)
C(43)	0.2774(10)	−0.1053(8)	−0.0198(10)
C(44)	0.3352(10)	−0.0571(8)	−0.0146(10)
C(45)	0.3405(10)	−0.0171(8)	0.0499(10)
C(46)	0.2821(9)	−0.0258(8)	0.1093(10)
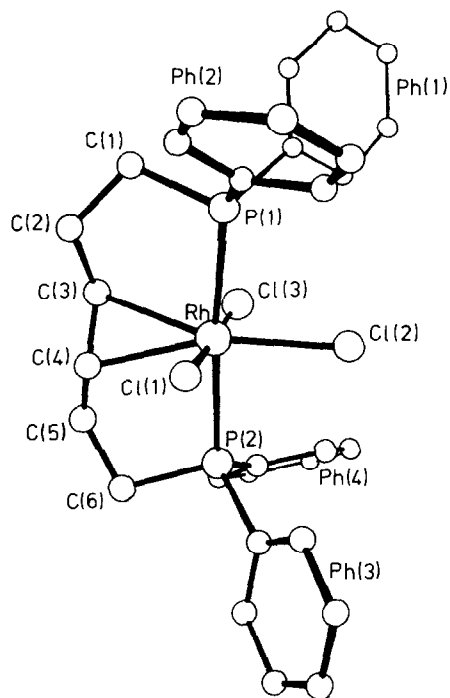
Fig. 1. Molecular geometry and atomic numbering for RhCl$_3$(BDPH).

Description and discussion of the crystal structures

Crystals of both complexes contain one monomer per asymmetric unit. The central metals are bonded to the BDPH moieties through the olefin and two phosphorus atoms, with the phosphorus atoms occupying mutually *trans* positions. The remaining sites in the slightly disordered octahedral arrangements are occupied by either three chloride ligands (Rh) or a carbonyl and two chloride ligands (Ru). In the latter case one chloride is situated *trans* to the olefin, whereas the remaining
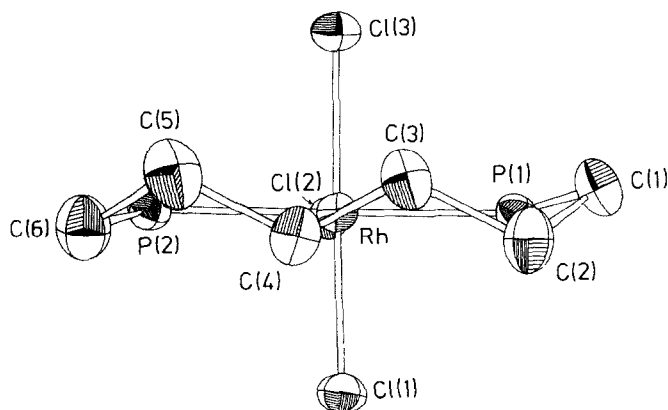

Fig. 2. Olefin orientation and anisotropic thermal ellipsoids (50% probability surfaces) for RhCl$_3$(BDPH).

TABLE 4

BOND DISTANCES (Å) AND ANGLES (°) FOR RhCl₃(BDPH)

Rh–Cl(1)	2.346(2)	Rh–P(1)	2.377(2)
Rh–Cl(2)	2.366(2)	Rh–P(2)	2.402(2)
Rh–Cl(3)	2.359(2)	Rh–C(3)	2.315(8)
Rh–C(4)	2.326(8)		
P(1)–C(1)	1.833(9)	P(2)–C(6)	1.826(9)
P(1)–C(11)	1.820(8)	P(2)–C(31)	1.827(8)
P(1)–C(21)	1.814(8)	P(2)–C(41)	1.830(8)
C(1)–C(2)	1.530(11)	C(4)–C(5)	1.489(12)
C(2)–C(3)	1.488(11)	C(5)–C(6)	1.502(12)
C(3)–C(4)	1.376(10)		
Cl(1)–Rh–Cl(2)	89.54(8)	Cl(2)–Rh–Cl(3)	91.14(8)
Cl(1)–Rh–Cl(3)	178.55(8)	Cl(2)–Rh–P(1)	86.25(7)
Cl(1)–Rh–P(1)	88.13(8)	Cl(2)–Rh–P(2)	88.62(7)
Cl(1)–Rh–P(2)	92.65(8)	Cl(2)–Rh–C(3)	162.1(2)
Cl(1)–Rh–C(3)	97.0(2)	Cl(2)–Rh–C(4)	163.3(2)
Cl(1)–Rh–C(4)	82.3(3)	P(1)–Rh–P(2)	174.81(8)
Cl(3)–Rh–P(1)	90.64(8)	P(1)–Rh–C(3)	77.4(2)
Cl(3)–Rh–P(2)	88.64(8)	P(1)–Rh–C(4)	107.9(2)
Cl(3)–Rh–C(3)	82.0(2)	P(2)–Rh–C(3)	107.6(2)
Cl(3)–Rh–C(4)	97.3(2)	P(2)–Rh–C(4)	77.3(2)
C(3)–Rh–C(4)	34.5(3)		
Rh–P(1)–C(1)	106.2(3)	Rh–P(2)–C(6)	105.9(3)
Rh–P(1)–C(11)	121.8(3)	Rh–P(2)–C(31)	121.6(3)
Rh–P(1)–C(21)	116.8(3)	Rh–P(2)–C(41)	113.2(3)
C(1)–P(1)–C(11)	103.9(4)	C(6)–P(2)–C(31)	104.5(4)
C(1)–P(1)–C(21)	105.1(4)	C(6)–P(2)–C(41)	105.1(4)
C(11)–P(1)–C(21)	101.3(4)	C(31)–P(2)–C(41)	105.1(4)
P(1)–C(1)–C(2)	106.0(6)	P(2)–C(6)–C(5)	106.5(6)
C(1)–C(2)–C(3)	107.3(7)	C(6)–C(5)–C(4)	109.7(7)
C(2)–C(3)–C(4)	124.3(8)	C(5)–C(4)–C(3)	125.4(8)
Rh–C(3)–C(2)	111.3(5)	Rh–C(4)–C(5)	110.8(6)
Rh–C(3)–C(4)	73.2(5)	Rh–C(4)–C(3)	72.3(5)

chloride and the carbonyl group are statistically disordered. The overall molecular geometries are illustrated in Figs. 1 and 2, while important bond lengths and angles are listed in Tables 4 and 5 respectively. Bond lengths and angles involving phenyl rings are available with the Supplementary Data.

In order to facilitate comparison with the previously published structure of the closely related compound IrCl₃(BDPH), the structures of IrCl₃(BDPH), RhCl₃-(BDPH) and RuCl₂(CO)(BDPH) will be described together.

Metal–chlorine and metal–carbonyl bonding

The M–Cl bond distances in the three complexes (mean values of 2.37, 2.35, 2.44 Å respectively [3]) fall generally within the range of observed M–Cl distances in similar complexes, e.g. Ir–Cl 2.361 Å in *mer*-(PMe₂Ph)₃IrCl₃ [11] and 2.34–2.38 Å in dichlorobis(ethylenediamine)Ir chloride [12], Rh–Cl 2.362 Å in *mer*-(PEt₂Ph)₃RhCl₃ [13] and 2.342, 2.346 Å in Rh(bdpps)Cl₃ [14]; RuCl 2.424(2) Å in

TABLE 5

BOND DISTANCES (Å) AND ANGLES (°) FOR $RuCl_2(CO)(BDPH)$

Ru–Cl(1)	2.436(4)	Ru–P(1)	2.388(4)
Ru–Cl(2A)	2.414	Ru–P(2)	2.416(4)
Ru–Cl(2B)	2.597	Ru–C(3)	2.30(1)
Ru–C(7A)	1.996	Ru–C(4)	2.32(1)
Ru–C(7B)	1.868	C(7A)–O(A)	1.359
C(7B)–O(B)	1.222		
P(1)–C(1)	1.84(2)	P(2)–C(6)	1.83(2)
P(1)–C(11)	1.84(2)	P(2)–C(31)	1.85(2)
P(1)–C(21)	1.83(2)	P(2)–C(41)	1.83(2)
C(1)–C(2)	1.55(2)	C(4)–C(5)	1.48(2)
C(2)–C(3)	1.46(2)	C(5)–C(6)	1.54(2)
C(3)–C(4)	1.37(2)		
Cl(1)–Ru–Cl(2A)	88.4	Cl(2B)–Ru–P(1)	92.4
Cl(1)–Ru–Cl(2B)	92 7	Cl(2B)–Ru–P(2)	86.3
Cl(1)–Ru–P(1)	86.9(1)	Cl(2B)–Ru–C(3)	80.8
Cl(1)–Ru–P(2)	89.2(1)	Cl(2B)–Ru–C(4)	95.0
Cl(1)–Ru–C(3)	161.8(4)	Cl(2B)–Ru–C(7B)	177.0
Cl(1)–Ru–C(4)	163.6(4)	P(1)–Ru–P(2)	175.7(1)
Cl(1)–Ru–C(7A)	89.5	P(1)–Ru–C(3)	76.5(4)
Cl(1)–Ru–C(7B)	90 3	P(1)–Ru–C(4)	107.3(4)
Cl(2A)–Ru–P(1)	88.2	P(1)–Ru–C(7A)	87.7
Cl(2A)–Ru–P(2)	93.2	P(1)–Ru–C(7B)	88.1
Cl(2A)–Ru–C(3)	98.3	P(2)–Ru–C(3)	107.2(4)
Cl(2A)–Ru–C(4)	83.9	P(2)–Ru–C(4)	76.9(4)
Cl(2A)–Ru–C(7A)	175.5	P(2)–Ru–C(7A)	90.7
C(3)–Ru–C(4)	34.6(5)	P(2)–Ru–C(7B)	93.5
C(3)–Ru–C(7A)	82 6	C(4)–Ru–C(7A)	99 2
C(3)–Ru–C(7B)	96.4	C(4)–Ru–C(7B)	82.1
Ru–C(7A)–O(A)	171.7	Ru–C(7B)–O(B)	175.3
Ru–P(1)–C(1)	107.0(5)	Ru–P(2)–C(6)	106.7(5)
Ru–P(1)–C(11)	121.9(5)	Ru–P(2)–C(31)	121.9(5)
Ru–P(1)–C(21)	117.4(5)	Ru–P(2)–C(41)	113.4(5)
C(1)–P(1)–C(11)	102.3(7)	C(6)–P(2)–C(31)	103.0(7)
C(1)–P(1)–C(21)	105.8(7)	C(6)–P(2)–C(41)	105.0(7)
C(11)–P(1)–C(21)	100.5(7)	C(31)–P(2)–C(41)	105.3(7)
P(1)–C(1)–C(2)	104.4(10)	P(2)–C(6)–C(5)	106.3(11)
C(1)–C(2)–C(3)	108.1(12)	C(6)–C(5)–C(4)	109.7(13)
C(2)–C(3)–C(4)	126.4(13)	C(5)–C(4)–C(3)	126.4(13)
Ru–C(3)–C(2)	113.7(10)	Ru–C(4)–C(5)	113.2(10)
Ru–C(3)–C(4)	73.6(8)	Ru–C(4)–C(3)	71.9(8)

$[RuCl(CO)_2(HNC_6H_5)(PPh_3)_2][ClO_4] \cdot CH_2Cl_2$ [15] and 2.415 Å (*trans* to C=C), 2.454 Å (*trans* to CO) in $RuCl_2(CO)(C_2H_4)(PMe_2Ph)_2$ [16]. The Ir–Cl and Rh–Cl bonds *trans* to the olefinic functions are slightly longer than those *trans* to the chlorine, implying a stronger structural *trans* influence of the olefinic ligand than that of a chloride ligand. This is consistent with other structural data on complexes containing olefin and chloride ligands [17]. The difference is more marked in the Ir case than the Rh. Iridium is a softer metal than rhodium and therefore may reasonably be supposed to bind to a greater extent to the olefinic moiety by both

stronger σ-donor and stronger π-acceptor modes. Consequent upon the strong σ-donation of the olefin to the iridium would be a weaker σ-donation from the *trans* chlorine ligand, and therefore a longer Ir–Cl bond. The slightly longer Ru–Cl bonds by comparison with the Ir– and Rh–Cl bonds could arise from the influence of the coordinated CO ligand (not present in the Ir and Rh complexes) or the effect of a lower positive charge on the metal centre (Ru^{II} compared with Ir, Rh^{III}) leading to weaker bonds to the chlorine ligands. Unfortunately, no firm conclusions can be made concerning the comparative effects of olefinic and carbonyl groups on *trans* ligands in the Ru complex because of the disorder problem associated with the chlorine and carbonyl ligand.

The BDPH ligand, and the metal–olefin bonding

The two metal–phosphorus bond lengths in each complex are slightly asymmetric (Ir–P 2.380, 2.390(2); Rh–P 2.377, 2.402(2); Ru–P 2.388, 2.416(4) Å; differences represent 5, 12 and 7 σ respectively), but all are typical values. Similarly, the carbon–carbon distances and angles in the alkyl chains of each ligand are normal values.

The metal–olefin coordinations are characterised by symmetrical bonding geometries, with comparatively long M–C bonds and comparatively short C=C bonds. The values in the Ir, Rh and Ru complexes are 2.271(10), 2.274(8), 1.350(13); 2.315, 2.326(8), 1.376(10); 2.30, 2.32(1), 1.37(2) Å. It can be seen that whereas the metal–P distances in all three complexes are very similar, the metal–carbon (olefin) distances are not as consistent.

In particular it can be noted in the case of Ir and Rh that if the equivalence of M–P distances reflects an equality in the covalent radii then the difference in the metal–olefin distances must imply a greater degree of metal–olefin backbonding in the Ir complex over that for Rh. This is also in agreement with the tendency for the Ir–Cl bond distances to be slightly longer than the Rh–Cl bond distances. Unfortunately the standard deviations in the C=C bond distances are too large for any definite conclusions to be made concerning the effect on the C=C bond of greater π-backbonding for the $IrCl_3$(BDPH) than for $RhCl_3$(BDPH). A comparison of the M–P and M–olefin distances for Rh^{III} and Ru^{II} would suggest that the degree of backbonding to the olefin is similar in these two complexes.

The structures of the Ir, Rh and Ru complexes described above were determined to afford a comparison with the known structures of IrH_2Cl(BDPH) (which was found to exhibit a very unusual metal–olefin coordination geometry, characterised by long Ir–C bonds (2.28, 2.34(2) Å), a short C=C bond (1.34(2) Å) and an intermediate olefin orientation) and IrCl(BDPH) (where the iridium(I)–olefin bonding was normal; Ir–C 2.084, 2.092(9), C=C 1.42(2) Å, olefin approximately perpendicular to the coordination plane). The long M–C and short C=C distances in the Ir^{III}, Rh^{III} and Ru^{II} complexes are consistent with a reduced extent of metal–olefin π*-backbonding compared with that in the Ir^I complex. This would be anticipated on the basis of a smaller number of electrons formally associated with the metals in the higher oxidation states. An important consequence of this decreased metal–olefin backbonding is the removal of the requirement that the olefin adopt an orientation perpendicular to the plane of the other donor atoms. In IrCl(BDPH) the short Ir^I–C distances implied a significant degree of metal–olefin backbonding, and the olefin was aligned approximately perpendicular to the square coordination plane [2]. In

IrCl$_3$(BDPH), RhCl$_3$(BDPH) and RuCl$_2$(CO)(BDPH), however, the reduced back-bonding has considerably weakened the metal–olefin bonding. This has allowed the olefins to adopt intermediate orientations of 28.2, 27.7 and 27.6° from the perpendicular direction (i.e. from the P–M–P axis). It has been suggested that the exceptionally large deviation of 49.8° noted in IrH$_2$Cl(BDPH) is due to a combination of the high oxidation state and further bond weakening influence of the hydride in the *trans* coordination site [2].

It is also pertinent to note that in the complex Mo(CO)$_3$(BDPH) the BDPH ligand also adopts a similarly twisted orientation (34.1°) even though the molybdenum is in a formal oxidation state of zero [4]. Here, the combined π-acceptor properties of the three carbonyl groups are sufficient on their own to reduce the strength of the Mo–olefin bonding.

References

1 P.W. Clark, J. Organomet. Chem., 137 (1977) 235.
2 G.R. Clark, M.A. Mazid, D.R. Russell, P.W. Clark and A.J. Jones, J. Organomet. Chem., 166 (1979) 109.
3 G.R. Clark, P.W. Clark and K. Marsden, J. Organomet. Chem., 173 (1979) 231.
4 G.R. Clark, C.M. Cochrane, P.W. Clark, A.J. Jones and P. Hanisch, J. Organomet. Chem., 182 (1979) C5; G.R. Clark, C.M. Cochrane and P.W. Clark, J. Organomet. Chem., 236 (1982) 197.
5 $\sigma(I) = \dfrac{20.1166}{NPI} \sqrt{C + 4B}$, where the constant term is the maximum possible scan rate, NPI is the ratio of the maximum possible scan rate to the scan rate for the measurement, C = total counts, B = total background.
6 All computing was carried out using the SDP suite of programs on a PDP-11 computer.
7 International Tables for X-ray Crystallography, Vol. IV, Kynoch Press, Birmingham, England, 1974. Tables 2.2B and 2.3.1.
8 $\sigma(F_o^2) = [\sigma(I_{raw})^2 + (p \times I_{raw})^2]^{1/2}/L_p$, where p is a fudge factor used to downweight intense reflections, I_{raw} = the observed intensity uncorrected for Lorentz polarization.
9 The final refined value of the extinction parameter g was 1.4794×10^{-7}. The expression used was $|F_c| = |F_o|(1 + gIc)$.
10 A.D. Booth, Fourier Technique in X-ray Organic Structure Analysis, Cambridge University Press, 1948, p. 62.
11 L. Aslanov, R. Mason, A.G. Wheeler and P.O. Whimp, J. Chem. Soc., Chem. Commun., (1970) 30.
12 A.E. Shvelashvili, A.I. Kvitashvili, M.N. Kandelaki and E.A. Mikeladze, Soobschch. Akad. Nauk. Gruz. SSR, 77 (1975) 361.
13 A.C. Skapski and F.A. Stephens, J. Chem. Soc., Dalton Trans., (1973) 1789.
14 G.B. Robertson, P.A. Tucker and P.O. Whimp, Inorg. Chem., 19 (1980) 2307.
15 F.A. Cotton and R. Eiss, J. Amer. Chem. Soc., 91 (1969) 6593.
16 L.D. Brown, C.F.J. Barnard, J.A. Daniels, R.W. Mawby and J.A. Ibers, Inorg. Chem., 17 (1978) 2932.
17 T.G. Appleton, H.C. Clark and L.E. Manzer, Coord. Chem. Rev., 10 (1973) 335; F.R. Hartley, Chem. Soc. Rev., 2 (1973) 163.